Journal of the Iranian Chemical Society (2022) 19:1191–1202
https://doi.org/10.1007/s13738-021-02374-x

ORIGINAL PAPER

Synthesis and characterization of cellulose nanofibers/chitosan/cinnamon extract wound dressing with significant antibacterial and wound healing properties

Amirhosein Kefayat[1] · Ramin Hamidi Farahani[1] · Mohammad Rafienia[2] · Ebrahim Hazrati[3] · Nafiseh Hosseini Yekta[4]

Received: 20 July 2021 / Accepted: 5 August 2021 / Published online: 12 August 2021

Abstract
Recently, bacterial cellulose-based wound dressings have gained lots of attention, and many studies have tried to improve the efficacy of these membranes with incorporation of different natural materials to fabricate an all-natural wound dressing with significant antibacterial and wound healing properties. In the present study, bacterial cellulose (BC) is produced from *Gluconacetobacter xylinus* to fabricate BC-based membranes. Then, chitosan (CS) and cinnamon extract (CE) are incorporated into the BC membranes to prepare an all-natural wound dressing. The obtained composite membrane (BC/CS/CE) is characterized according to chemical properties, surface morphology, mechanical properties, water absorptivity, water retention, CE release, antibacterial activity, biocompatibility, in vivo wound healing activity, and compared with BC and BC/CS membranes. The BC/CS/CE membrane is able to maintain appropriate moisture content for an acceptable period of time. Although the tensile strength and elongation at break values of the BC/CS/CE are slightly lower than the BC membrane, they are still in ideal ranges. The BC/CS/CE membrane exhibits significantly more antibacterial effects against *Staphylococcus aureus* and *Escherichia coli* in comparison with the BC and BC/CS which can be related to the sustained released profile of CE. In addition, BC/CS/CE is more biocompatible with L929 normal skin fibroblast cells in comparison with the BC and BC/CS membranes. Also, the BC/CS/CE membrane can meaningfully promote the wound healing progress compared with other membranes at the Wistar rats full-thickness skin wound model. The BC/CS/CE membrane-treated wounds have more developed dermis layer in comparison with other groups according to histopathological analyses. Taking together, the CS and CE enriched BC membranes can be a promising wound dressing with desirable properties.

Keywords Wound dressing · Cellulose · Cinnamon extract · Chitosan · Antibacterial properties

Abbreviations

BC	Bacterial cellulose
CE	Cinnamon extract
CS	Chitosan
H&E	Hematoxylin & Eosin

✉ Ramin Hamidi Farahani
rgsramin@yahoo.com

[1] Department of Infectious Diseases, Faculty of Medicine, AJA University of Medical Sciences, Tehran, Iran

[2] Biosensor Research Center, Isfahan University of Medical Sciences, Isfahan, Iran

[3] Department of Anesthesiology and Intensive Care, Faculty of Medicine, AJA University of Medical Sciences, Tehran, Iran

[4] Department of Persian Medicine, Faculty of Medicine, AJA University of Medical Sciences, Tehran, Iran

Introduction

Skin plays a key role in protecting the human body from microbial invasion, loss of fluid, and other vital components. It, as the largest human body organ, is always at the exposure to different physical and thermal injuries [1]. A wound is defined as a disruption in the skin epithelium continuity and can severely affect patients' life and health, especially the extensive full-thickness wounds due to taking longer time for repair [2, 3]. Therefore, wound dressings with significant ability to promote the wound healing process and prevent wound infection are highly needed.

Wound dressings consisted of synthetic polymers exhibit a vast variety of limitations including low biocompatibility, high risks of inflammation and infections, especially after long-term use. Thus, using natural polymers (cellulose, chitosan, hyaluronic acid, etc.) for fabricating wound dressings, has gained lots of attention due to their high

biocompatibility, availability, absorbability, versatility, and possible similarity to the structure of the extracellular matrix [4, 5]. One of the most well-known natural polymers with promising potential for wound dressings is bacterial cellulose (BC). This nanoscale cellulose exhibits significant physicochemical and mechanical properties, outstanding biocompatibility, and biodegradability [6]. In addition, many studies have reported its high capacity for retaining moisture and absorbing exudates from the injured tissue and accelerate the granulation process [7, 8]. Moreover, BC exhibits some advantages over plant-derived cellulose like high purity, simple purification process, and three-dimensional network structure similar to the extracellular matrix which has caused considerable employment of this biopolymer for fabricating wound dressings [9–11]. Although cellulose has many excellent properties for wound healing, the lack of antimicrobial activity is an obvious limitation of cellulose-based wound dressings. Thus, different materials with antibacterial properties should be incorporated into these wound dressings to prevent wound infection [12].

Chitosan (β-1,4-linked glucosamine) is the second most abundant biopolymer after cellulose and is derived from crustaceans' outer shells [13]. Some of its biological properties such as biodegradability, biocompatibility, antibacterial activity, scar prevention, cell affinity, and anti-inflammatory effects, making it an ideal candidate for the fabrication of wound dressings [9, 14–16]. Chitosan (CS) exhibits significant antimicrobial activity against various microorganisms, such as bacteria, fungi, yeasts, and viruses [17]. Its antimicrobial effects are related to the permeabilization of the microbial plasma membrane. It was also reported that CS can destabilize the outer membrane of Gram-negative bacteria and chelate their endotoxins to decrease their acute toxicity [18, 19]. Also, its anti-inflammatory effects can control prolonged inflammation at the wound site which can accelerate the healing process [20].

The use of plant extracts for the treatment of burns and wounds is a common practice followed over the decades [21]. Many medicinal plants have a long history of curative properties in wound healing. *Cinnamomum zeylanicum*, generally known as cinnamon, is one of the most well-known medicinal plants for wound healing. According to recent studies, cinnamon exhibits significant anti-bacterial and anti-fungal properties, which are deeply related to its phenolic compounds [22–24]. These compounds disrupt microorganism cell membranes and their structures which leads to ion leakage [25, 26]. Many studies identified cinnamaldehyde as one of the most responsible compounds for the major antibacterial activities of cinnamon [26]. Trans-cinnamaldehyde is also known to inhibit bacterial acetyl-CoA carboxylase [27]. Systemic or topical administration of cinnamon extract causes significant wound healing promotion effects in animal skin wounds models and enhances wound contraction, re-epithelialization, keratin biosynthesis, and skin regeneration [28–30]. So many studies have reported the incorporation of cinnamon extract (CE) into the wound dressing to enhance its efficacy in different aspects [31–33].

In the present study, a BC-based membrane was produced from *Gluconacetobacter xylinus*. Then, cinnamon extract and chitosan were incorporated into the BC membranes to prepare an all-natural novel wound dressing with antibacterial and wound healing activities. The morphology, mechanical properties, water absorptivity, water retention, cytocompatibility, and antibacterial activities of the prepared membranes (BC, BC/CS, and BC/CS/CE) were assessed. Also, the wound healing properties of the membranes were evaluated in the Wistar rats full-thickness skin wounds model.

Materials and method

Materials

Cinnamon bark was collected from local stores. Ethanol, chitosan (Mw 1000 kDa, 85% degree of deacetylation (DD)), and acetic acid were purchased from Sigma-Aldrich. The cell culture materials including RPMI, penicillin–streptomycin solution, fetal bovine serum (FBS), 0.05% trypsin/EDTA, and phosphate buffer saline (PBS) were bought from Bioidea. The MTT assay kit was purchased from Sigma-Aldrich. *Staphylococcus aureus* (ATCC 25,923), *Gluconacetobacter xylinus* (ATCC 10,245), *Escherichia coli* (ATCC 25,922), L929 fibroblast cell line, Wistar rats were purchased from the Pasteur Institute of Iran, Tehran.

Cinnamon extract preparation

The CE was prepared according to the previous studies [31]. Laboratory ceramic porcelain mortar and pestle were employed to ground cinnamon bark into small grains (particle size ~ 3 mm). The cinnamon particles were added to a Soxhlet extractor with 500 mL capacity. The extraction procedure was performed with 250 mL ethanol for 2 h. Subsequently, a rotary evaporator was used to evaporate 90% of the initial volume of the resulting dark brown solution at 50 °C. The residual solvent was evaporated using a freeze dryer (−60 °C, 5 mbar, 48 h). The final extract was stored at -20 °C until further use.

Membranes preparation

G. xylinus (ATCC 10,245) bacterial strain was used for the BC production. The previous studies protocol was used with slight modifications [34, 35]. The Hestrin and Schramm culture medium (2.0% (w/v) glucose, 0.5% (w/v) peptone,

0.5% (w/v) yeast extract, 0.27% (w/v) disodium phosphate, 0.115% (w/v) citric acid) was prepared, and its pH was adjusted to 5.0. The sterilized medium was inoculated with *G. xylinus* (5–10%, v/v) and cultivated statically for one week. The celluloses were collected and rinsed with deionized water several times to remove bacteria and nutrients. The wet BC membranes were then sterilized by autoclaving, and a compressor was employed to compress them for removing excess water. Finally, the membranes were freeze-dried, and the dry BC membranes with the final thickness of 0.1–0.15 mm were stored at room temperature. To prepare bacterial cellulose-based membranes incorporated with CS, CS was dissolved in a 1% v/v citric acid aqueous solution so the concentration of CS in the solution was 0.6% w/v. Wet BC membranes were then immersed in the CS solution for 12 h. The end product was freeze-dried and abbreviated as BC/CS. To prepare bacterial cellulose-based membranes incorporated with CS and CE, CE was dissolved in 1% v/v citric acid so the concentration of CE in the solution was 5% w/v. Then, CS was dissolved in the solution to reach a 0.6% concentration in the solution. A magnetic stirrer was employed to have a homogeneous solution. Wet BC membranes were then immersed in the resultant solution for 12 h. The end product was freeze-dried and abbreviated as BC/CS/CE.

Attenuated total reflectance/Fourier transform infrared spectroscopy (ATR/FTIR)

The infrared spectroscopy technique is a well-known technique for characterizing the chemical composition of membranes and the possible interactions between their composing components. The analysis was performed using an attenuated total reflectance (ATR) cell on the spectrophotometer FTIR-4200 type A (JASCO, Japan) in a wavenumber ranging from 600–4000 cm^{-1}, at ambient temperature with 4 cm^{-1} resolution and 64 scans.

Morphology assay

Surface morphologies of the BC, BC/CS, and BS/CS/CE scaffolds were showed by scanning electron microscope (SEM) (Philips XL30, Netherlands) at an accelerating voltage of 10 kV. Samples were coated with a thin layer of gold and then observed by SEM.

Water absorptivity assay

The water absorptivity of membranes was assessed according to the previous studies [36]. At first, 4 cm × 4 cm pieces from the membranes were prepared. The dry weight of these pieces was precisely measured (Wdry). The samples were immersed in deionized water (30 mL, 25 °C). Subsequently, the membranes were withdrawn from the water at a specific time point to measure their wet weight (Wwet). Before weighting, a filter paper was employed to remove the excess surface water. Equations (1) and (2) are used to calculate the swelling ratio and moisture content ratio of the membranes, respectively. These tests were repeated at least four times.

$$\text{Swelling ratio } (\%) = \frac{Wwet - Wdry}{Wdry} \times 100 \quad (1)$$

$$\text{Moisture content ratio } (\%) = \frac{Wwet - Wdry}{Wwet} \times 100 \quad (2)$$

Water retention assay

At first, the initial dry weight (Wdry) of the membranes was measured. These dried membranes were immersed in deionized water. After 24 h, the swollen membranes were withdrawn from the water and a filter paper was employed to remove the excess water on the surface of the membranes. Then, the membranes were placed in open mouth dishes at room temperature. After a specific time period, the specimens were taken out and weighed (Wwet) again. Equation (3) is used to calculate the water retention ratio.

$$\text{Water retention ratio } (\%) = \frac{Wwet - Wdry}{Wdry} \times 100 \quad (3)$$

Mechanical test

The mechanical properties of membranes' were assessed according to our previous study [37]. Instron Universal Testing Machine (Instron Engineering Corporation, Canton, MA, USA) equipped with a load cell of 100 N was used for this purpose. Strips with 10 mm width and 30 mm length were prepared from the membranes. All measurements were preload of 0.1 MPa with a crosshead speed of 5 mm/min at ambient temperature. The values were obtained from 6 measurements.

CE release

The CE release profile of the BC/CS/CE composite membrane was assessed according to previous studies [31]. Briefly, a 2 × 2 cm^2 piece of the membrane was cut, precisely weighed, and then placed in a glass bottle containing 5 mL PBS solution. The bottle temperature was kept at 37 ± 0.1 °C using a water bath. Subsequently, 1 mL of the solution was collected at different time intervals (1, 2, 4, 8, 16, 24, 48, 72, 96, 120, and 144 h) for later assessments. At each time interval, the lost volume was compensated by adding 1 mL of fresh PBS solution to the bottle. The collected samples were mixed with

3 ml ethanol and then centrifuged at 4000 rpm for 10 min. At last, an array UV/Vis spectrophotometer was used to record the spectrum of the sample at 180–700 nm wavelengths.

Antibacterial activity assay

Zone of inhibition (ZOI) test was used to assess the antibacterial activity of the BC, BC/CS, and BC/CS/CE membranes. *Staphylococcus aureus* (ATCC 25923) and *Escherichia coli* (ATCC 25922) as two of the most common wound infection-associated pathogens were used for this purpose [38]. Nutrient agar medium was prepared and sterilized according to our previous study [39]. 100 µL of bacteria containing medium after overnight incubation was spread over the nutrient agar medium by a glass L-rod. The samples were placed over the medium and incubated at standard condition. After 24 h, the clearance zones around the discs were measured by a digital caliper. The test was done in triplicate.

Cell viability assay

Biocompatibility of the BC, BC/CS, and BC/CS/CE dressings with L929 murine fibroblast cells was evaluated using the colorimetric MTT assay. Samples with 4 cm^2 area were prepared from each membrane and sterilized through 2-h UV light irradiation. The sterilized samples were placed into the cell culture plates wells which contained RPMI and were incubated for 1, 3, and 7 days at standard cell culture conditions (37 °C, 95% relative humidity, and 5% CO2). On each of the specified days, 100 µL of the incubated cell culture medium was transferred into a 96-well cell culture plate. 5×10^3 L929 cells which were suspended in standard cell culture media (RPMI media supplemented with 15% fetal bovine serum and 1% penicillin/streptomycin) were added to each well. The plate was then incubated for 24 h. Then, the culture media was discarded, and wells were washed with PBS. A basal culture medium containing 0.005% MTT solution was added. After 4-h incubation (37 °C, 5% CO2) in the dark, the content of each plate was substituted with 200 µL of DMSO. Finally, the absorbance of each well was detected by an Absorbance Microplate Reader (BioTek-ELX800, USA) at the wavelength of 570 nm. According to Eq. (4), the percentage of cell viability was calculated by relative value to the untreated cells as the control group. The experiment was repeated three times:

$$\text{Cell Viablity}(\%) = \frac{OD\ \text{Sample} - OD\ \text{Blank}}{OD\ \text{Control} - OD\ \text{Blank}} \times 100 \qquad (4)$$

Animal skin wound model

In total, 32 female Wistar rats (200–250 g) were purchased from the Pasteur Institute of Tehran, Iran. All animal experiments and protocols were approved by the ethical committee of the AJA University of Medical Sciences (IR.AJAUMS.REC.1398.263). The animals were kept at the standard condition with complete access to standard laboratory animals' food and water. They were acclimated for two weeks before entering any experiment. On the day of operation, the animals initially were completely anesthetized by intraperitoneal injection of ketamine (100 mg/kg) and xylazine (10 mg/kg) mixture. The surgery site (the animals' dorsal region skin) was completely shaved by an electric shaver and then disinfected using alcohol 70%. Subsequently, round excisions (11 mm in diameter) were made on the back of the rats using a punch biopsy. Then, the animals were randomly divided into four groups (n = 8) including control, BC, BC/CS, and BC/CS/CE. For the control group, sterile cotton gauze was applied to the wound. For other groups, the related wound dressings were applied precisely on the wound site and sterile cotton gauze was applied on the wound site. Each rat was kept in separate cages. To manage postoperative pain, ketoprofen (5 mg/kg) was administered subcutaneously until 72 h after operation. The operation day was accounted as 1st day, and the wound healing process was evaluated by measurement of wound diameters at 1^{st}, 5^{th}, and 10^{th} days by a digital caliper. The percentage of the wound area closure was calculated by Eq. (5) [2–4]. It should be mentioned that standardized humane endpoints based on the current guidelines for endpoints in animal studies were used [36, 40, 41].

$$\text{Wound area closure}(\%) = \frac{\text{Wound area at the first day} - \text{Wound area at day}\ (n)}{\text{Wound area at the first day}} \times 100 \qquad (5)$$

Histopathological analysis

The animals were killed by ketamine-xylazine mixture overdose on the 10^{th} day after wound creation. Then, full-thickness skin excisions were made from the wound area (n = 8). The skin specimens were fixed in 10% formalin neutral buffer solution for 24 h. The fixed specimens were processed by an automatic tissue processor (Sakura, Japan). Then, 4-µm-thick serial sections from the paraffin-embedded blocks were prepared by a microtome (Leica Biosystems, Germany). The sections were stained with hematoxylin & eosin (H&E) staining protocols for subsequent histological evaluation [42]. The mounted slides were observed under a digital light microscope (Olympus, Japan) which was equipped with an Olympus DP70 digital camera.

Statistical analysis

The quantitative data were displayed as mean ± standard deviation (SD). Statistical analyses for elucidating differences between groups were conducted using one-way analysis of variance (ANOVA) and Tukey's HSD post hoc test by SPSS software V.23. The difference was considered statistically significant if $P < 0.05$. (*: P ˂ 0.05).

Results and discussion

Morphology of the membranes

The surface morphology of the BC, BC/CS, and BC/CS/CE membranes was investigated by SEM. As Fig. 1A illustrates, the BC membrane was composed of randomly arranged nanofibers which designed a disciplined network and some empty space and pores in-between. Yano et al. [43] reported that the bacteria polymerize glucose molecules through β–(1 → 4) glucan chains and excrete the polymer to the extracellular space to form nanofibrils that are further organized and stabilized by intramolecular hydrogen bonds to generate an ultrafine reticulated structure. As Fig. 1B and C shows, the BC/CS and BC/CS/CE composite membranes were even more compact than the BC membrane probably and exhibited a smoother surface than the BC membrane which can be attributed to the presence of chitosan on the surface. It has been previously reported that chitosan can enter the bacterial cellulose's pores and interact with the nanofibrils, which may affect physical and chemical properties of the fabricated membrane [44]. Our observations were consistent with the Lin et al. [34] study results which reported that chitosan incorporates with the BC membranes' nanofibrils and forms a denser network structure, and decreases the porosity of membrane. Also, the addition of CE is not changing the smooth morphological of BS/CS.

FTIR studies

To confirm the formation of the composite membranes, the FTIR spectra of CS, CE, BC membrane, BC/CS, and BC/CS/CE composite membranes were evaluated in different steps (Fig. 2). At first, FTIR spectra were obtained for BC (Fig. 2A), CS (Fig. 2B), and CE (Fig. 2C). The FTIR spectrum of BC indicates characteristic absorption bands at 3339 cm^{-1} and 3241 cm^{-1} corresponding to stretching vibrations of O–H stretch from hydroxyl groups. The peaks in the 2863–2891 cm^{-1} region are related to the C–H stretching from methyl and methylene groups. Other peaks in the range of 1424–1451 cm^{-1} are due to the –CH2 scissoring motion in cellulose. Also, 1365 cm^{-1} and ~ 1315 cm^{-1} represent the C–H bending and CH2 wagging, respectively. The sugar ring absorptions at 1059, 1029, 1105, 1158 and 1203 cm^{-1} are corresponding to the C–O–C ether stretching vibration, and O–H vibrations belong to the primary and secondary hydroxyl bendings [45]. The FTIR spectrum of CS shows a strong band in the 3385–3424 cm^{-1} region related to N–H and O–H stretching and also, the intramolecular hydrogen bonds. The absorption bands at 2922 and 2880 cm^{-1} may be due to symmetric and asymmetric C-H stretchings, respectively. These bands are characteristics of polysaccharide spectra. Absorption bands at 1656 cm^{-1} (C = O stretching of amide I) and 1324 cm^{-1} (C-N stretching of amide III) are related to the residual N-acetyl groups. A band at 1598 cm^{-1} can be attributed to the N–H bending of the primary amine. Moreover, vibrational peaks at 1423 cm^{-1}, 1380 cm^{-1}, 1156 cm^{-1}, and 1076–1032 cm^{-1} are related to CH2 bending, CH3 symmetrical deformations, asymmetric C–O–C bridge, and C-O stretching [31, 46]. FTIR spectrum of CE includes different chemical compounds such as hydroxycinnamic acid, hydroxyl cinnamaldehyde, and cinnamaldehyde. The peaks observed at 3370 cm^{-1}, 2974–2894 cm^{-1}, 2752 cm^{-1}, 2133 cm^{-1}, 1757 cm^{-1}, 1662 cm^{-1}, 1618 cm^{-1}, and 1481 cm^{-1} are

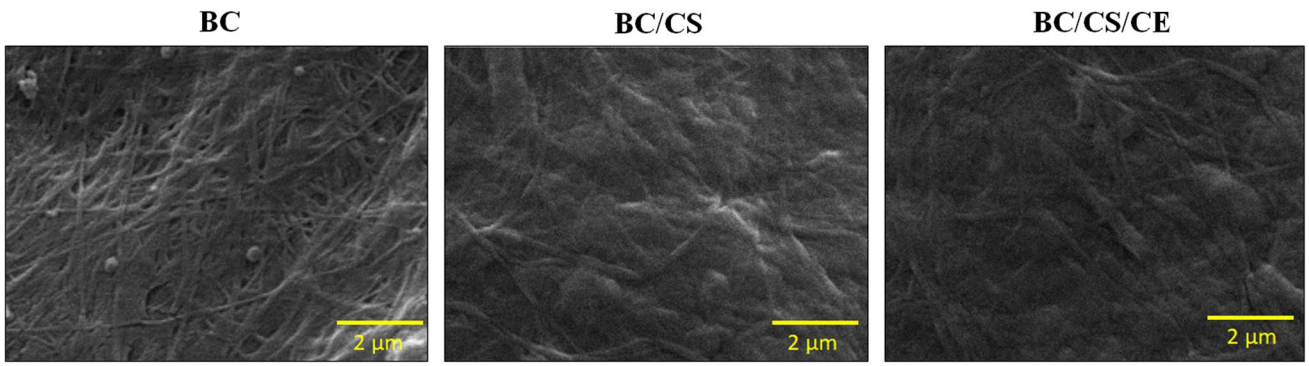

Fig. 1 SEM photographs of the BC, BC/CS, and BC/CS/CE membranes. Magnification: 40,000×, HV: 10.00 kV, Vac mode: high vacuum, WD: 10.2 mm

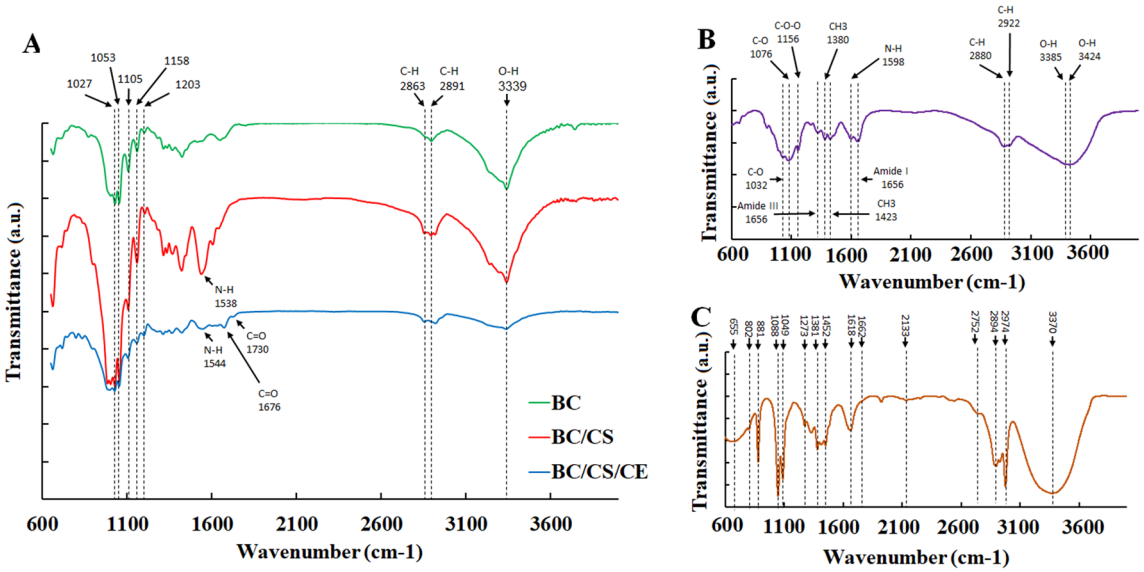

Fig. 2 FTIR spectra of the (A) BC, BC/CS, and BC/CS/CE membranes, (B) CS, (C) CE

representative of phenolic O–H stretching of alcohols and phenols, vibration stretch C–H sp3 of alkanes, C-H aldehyde, –C≡C– stretch of alkynes and aldehydes, stretch aldehyde C = O of saturated fat, C = O stretch cinnamaldehyde (conjugated) that is a dominant component of cinnamon, C = C conjugated with an aromatic ring, and C = C aromatic groups, respectively. In the fingerprint region, 1452–1381 cm^{-1}, 1273 cm^{-1}, 1088–1049 cm^{-1}, 881 cm^{-1}, 802 cm^{-1}, and 655 cm^{-1} peaks are related to the C-H out-of-plane bending of CH3 group, C–O stretch for phenol hydroxyl, C–O stretch for aliphatic amines, sp3 C–H bending, sp2 C–H bending aromatic, and C≡C-H bending of alkynes and alky1 absorption. This can demonstrate the presence of cinnamon, aldehydes, and cinnamaldehyde as recently reported [31, 47].

At the second step, FTIR spectra were recorded for the BC/CS and BC/CS/CE and compared with BC, CS, and CE in the pure state. With respect to the obtained results, the presence of CS and CE in cellulose nanofibers could be well confirmed. In this regard, the sugar ring absorptions which belong to BC (1027, 1053, 1105, 1158, and 1203 cm^{-1}) can be observed for both BC/CS and BC/CS/CE. Also, peaks of the BC functional group can be observed for these two composite membranes. Moreover, the presence of CS is well demonstrated by the characteristic band corresponding to the N–H bending of the primary amine which was observed at 1538 cm^{-1} in BC/CS and 1544 cm^{-1} in the BC/CS/CE spectrum. Finally, the presence of CE in the BC/CS/CE composite membrane could be obviously confirmed by stretch aldehyde C = O centered at 1676 cm^{-1} and 1730 cm^{-1} that belong to the saturated fat and cinnamaldehyde as a major component of cinnamon, respectively. Taking together, these FTIR analyses can demonstrate the successful synthesis of BC/CS/CE as an all-natural composite membrane for wound healing application.

Water absorptivity and retention properties

Wound moisture is very important due to its determinative effect on increasing active substances penetration to the wound site, inhibition of microorganism invasion, and decreasing the pain of wound dressing removal from the wound surface [48]. Therefore, an appropriate wound dressing should be able to absorb the wound exudate, as well as keeping a moist environment at the wound site along the healing process. The swelling profile, moisture content, and water retention capacity parameters were assessed to represent these abilities of the BC, BC/CS, and BC/CS/CE wound dressings. As Fig. 3A and B illustrates, all the membranes exhibited high saturation with water after immersing in the deionized water for 24 h. In addition, the BC/CS and BC/CS/CE composite membranes exhibited lower swelling ratio (Fig. 3A) and moisture content ratio (Fig. 3B) compared with the BC membrane. This can be related to CS incorporation into the BC membrane as previous studies have reported that incorporation of chitosan into the nanofibers of BC membranes forms a denser network structure and decreases the porosity of BC membrane [34, 44]. On the other hand, BC, BC/CS, and BC/CS/CE membranes did not exhibit any significant difference at water retention parameter (Fig. 3C).

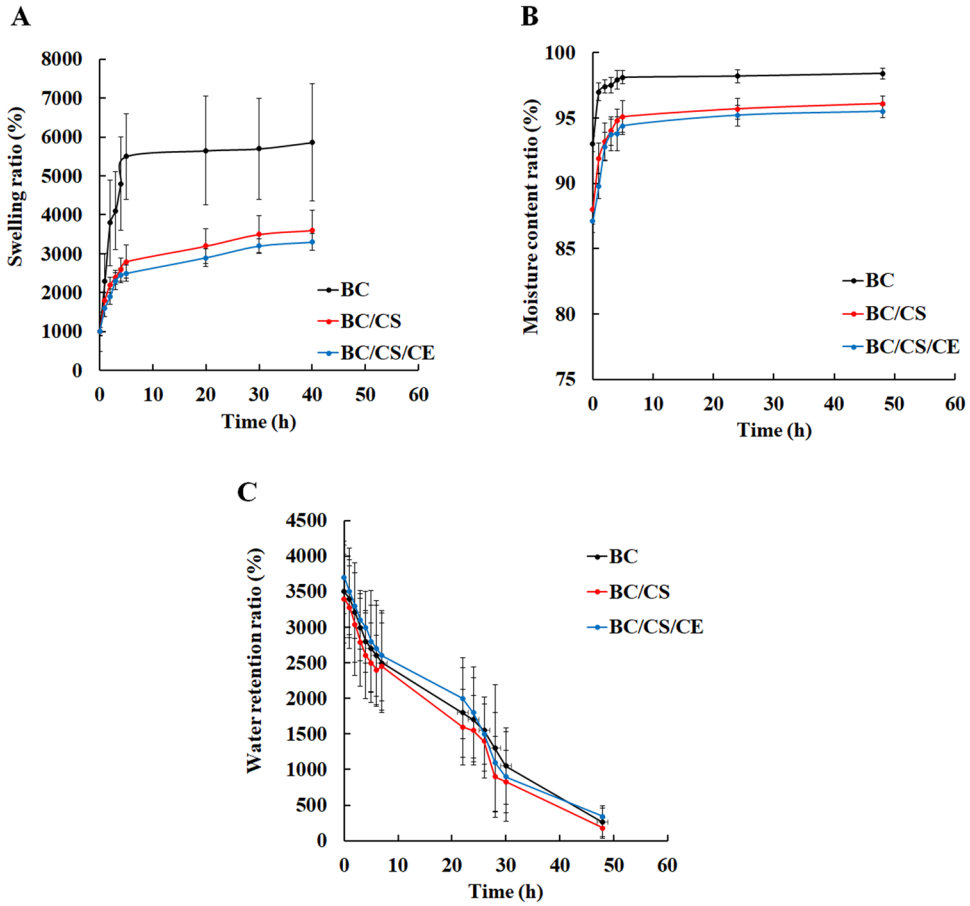

Fig. 3 (**A**) Swelling ratio, (**B**) moisture content ratio, (**C**) water retention ratio of the BC, BC/CS, and BC/CS/CE membranes

Table 1 Mechanical properties of the BC, BC/CS, BC/CS/CE membranes

Sample	Tensile strength (MPa)	Elongation at break (%)
BC	20.2 ± 3.8 [a]	45.6 ± 10.8 [a]
BC/CS	16.9 ± 5.4 [a]	39.8 ± 6.2 [a]
BC/CS/CE	15.3 ± 6.7 [a]	42.7 ± 7.8 [a]

Values represent mean ± standard deviation. In each column, values not connected by the same letters are significantly different ($P < 0.05$)

Mechanical properties

The handling quality and the ability to maintain the integrity during use for a wound dressing can be assessed by the mechanical properties. As Table 1 shows, the elongation at break of the BC, BC/CS, and BC/CS/CE membranes was 45.6 ± 10.8%, 39.8 ± 6.2%, 42.7 ± 7.8%, respectively. Also, the tensile strength of the BC, BC/CS, and BC/CS/CE membranes was 20.2 ± 3.8 MPa, 16.9 ± 5.4 MPa, and 15.3 ± 6.7 MPa, respectively. Although CS and CE incorporation did not cause a statistically significant effect ($P > 0.05$) on the mechanical properties of BC samples, the mechanical properties of composite membranes (BC/CS and BC/CS/CE) were in an appropriate range for a wound dressing according to previous studies [34, 37].

CE release profile

As Fig. 4 illustrates, the CE release profile of the BC/CS/CE composite membrane exhibited a burst release, followed by a sustained and prolonged form of release. The burst release phase was observed in about 8, and almost 51% of the CE was released (Fig. 4A), which may be attributed to the proportion of CE that is physically absorbed on the surface of the fibers of BC/CS/CE membrane. The latter phase was detectable after 8 h (Fig. 4B), and until day 6, about 71% of the extract was released. This phase exhibited a favorable slow, sustained, and prolonged form of release which can sustain all the beneficial effects of CE (such as antibacterial, pro-wound healing, and hemostatic effects) at the wound site during the healing process [49, 50].

Antibacterial activity

Wound infection can disrupt the healing process. But the most important concern about wound infection is the possibility of forming sepsis. Thus, antibacterial activity is a

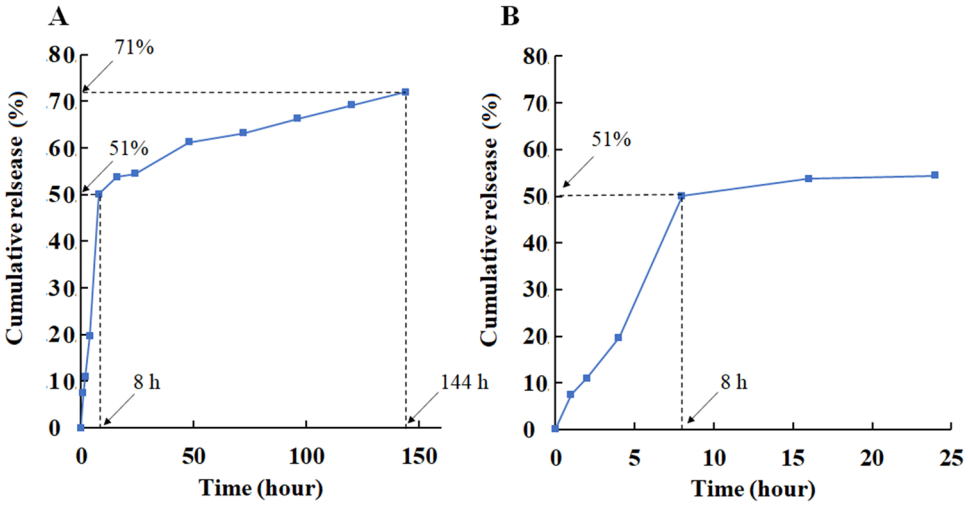

Fig. 4 (**A**) Cumulative release of CE from the BC/CS/CE membrane in 144 h (6 days). (**B**) Magnification of the first 24 h part of the cumulative release curve

Table 2 Antibacterial activity of the BC, BC/CS, BC/CS/CE membranes according to the zone of inhibition test

Microorganism	BC	BC/CS	BC/CS/CE
E. coli	0	0.9 ± 0.24	2.18 ± 0.39
S. aureus	0	4.26 ± 0.43	6.13 ± 0.72

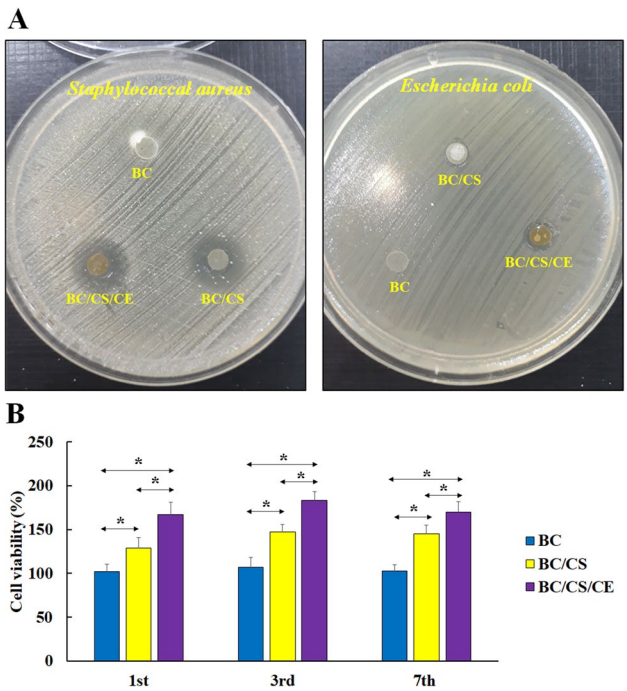

Fig. 5 (**A**) The antibacterial activity of the BC, BC/CS/ BC/CS/CE membranes against *Staphylococcal aureus* and *Escherichia coli* strains according to the zone of inhibition test. (**B**) Biocompatibility of the BC, BC/CS/ BC/CS/CE membranes with L929 skin normal fibroblast after different incubation times (1, 3, and 7 days) according to MTT assay analyses (*: $P < 0.05$, ns: not significant)

determinative parameter for any wound dressing [51]. The zone of inhibition test was used as a well-known method to assess the antibacterial effects of membranes against *Staphylococcal aureus* and *Escherichia coli* which are two of the most common wound infection-associated pathogens [38]. The BC membrane did not form any inhibition zone which indicates that BC membrane per se has no antibacterial effects (Table 2, Fig. 5A). This fact has been widely mentioned by multiple studies as a big weakness point of BC-based membranes for constructing a wound dressing. However, incorporation of CS into the BC membrane caused rising some antibacterial effects at the BC/CS composite membrane. The antibacterial effects of CS can be attributed to two well-known mechanisms of action. The first one is the interaction of positively charged CS with the negatively charged portions of bacteria surface which increases bacteria membrane permeability and inhibits their growth. On the other hand, the binding of chitosan to the DNA can disrupt mRNA generation in bacterial cells [34, 52]. The highest antibacterial activity among all the samples was observed at the BC/CS/CE composite membrane which demonstrates the importance of CE. Many studies have identified cinnamaldehyde as the main responsible chemical component of CE for its antibacterial properties [53, 54]. The BC/CS/CE membrane caused significantly lower antibacterial activity against *E. coli* in comparison with *S. aureus*. Zhang et al. [55] reported the same observation and related the reason for this observation to the structural difference in these two bacterial strains' outer shell. The cell wall of *E. coli* is covered by a thick membrane of lipopolysaccharide, while *S. aureus* has a single peptidoglycan layer [55, 56]. So, *E. coli* exhibits more resistance to hydrophobic antibacterial agents like CE [31]. Taking together, not only the BC/CS/CE composite membrane has significant antibacterial activity, but the wound site will also remain free of

bacteria due to the continuous release of CE from the BC/CS/CE wound dressing.

Cellular biocompatibility

Biocompatibility of wound dressing with skin fibroblast is another determinative parameter for their efficacy [7]. As Fig. 5B illustrates, the BC membrane was completely biocompatible with the skin normal fibroblast cells (L929 cell line). Significant ($P < 0.05$) increase in the proliferation rate of these cells was observed just at the BC/CS and BC/CS/CE composite membranes at all time intervals. Also, the highest increase in the cells' proliferation was observed at BC/CS/CE composite membrane. These results demonstrate the significant benefits of incorporating CS and CE into the BC membrane for enhancing skin normal fibroblast cells proliferation. The related mechanism by which CS activates and increases proliferation in the normal fibroblast cells is still unknown. But some studies reported that the high binding ability of CS to the serum growth factors may prevent their degradation or perhaps has activating effects which stimulate cells proliferation [57]. On the other hand, the addition of CE into the BC/CS membrane to form the BC/CS/CE increases the proliferation activating effects of this composite membrane. The most recommended concentration for CE incorporation into the wound dressings is 5% according to previous studies. Many studies observed decreased cell viability at CE contents higher than 5% [31, 33, 58]. Therefore, in this study 5% CE content was used to prepare the BC/CS/CE composite membrane, and significant proliferation activating effects on the normal skin fibroblast cells and inhibitory effect on the bacterial growth and proliferation were detected.

In vivo *wound healing assessment*

The membrane's ability to promote the wound healing process was assessed in the Wistar rats' full-thickness skin wound model. The wounds were treated with gauze as control, BC, BC/CS, and BC/CS/CE membranes in different groups (n = 8). No evidence of skin necrosis, wound complication, or animal death was observed at the treatment groups during follow-up. As Fig. 6A illustrates, the wound at the BC/CS/CE was completely closed after 10 days from the operation, while wound at the other groups was still unhealed. As Fig. 6B illustrates, at both time points (5^{th} and 10^{th} days), the BC/CS/CE group exhibited significantly ($P < 0.05$) more accelerated wound closure rate compared with the control, BC, and BC/CS treated groups. These findings are consistent with histological investigations of the wounds on the 10^{th} day which is illustrated in Fig. 6C. The wounds treated with the BC/CS/CE composite membrane exhibited more developed epidermis and dermis, hair follicles, sebaceous glands formation, arranged collagen fibers at the dermis layer, and integrated keratin formation in comparison with other treatment groups on the 10^{th} day [7, 37]. Therefore, significantly higher wound healing activity was detected at BC/CS/CE wound dressing treated group in comparison with BC and BC/CS groups. Lin et al. [59] evaluated the bacterial cellulose/chitosan membranes effect on the *Sprague Dawley* rats' skin wound model. Their bacterial cellulose was produced

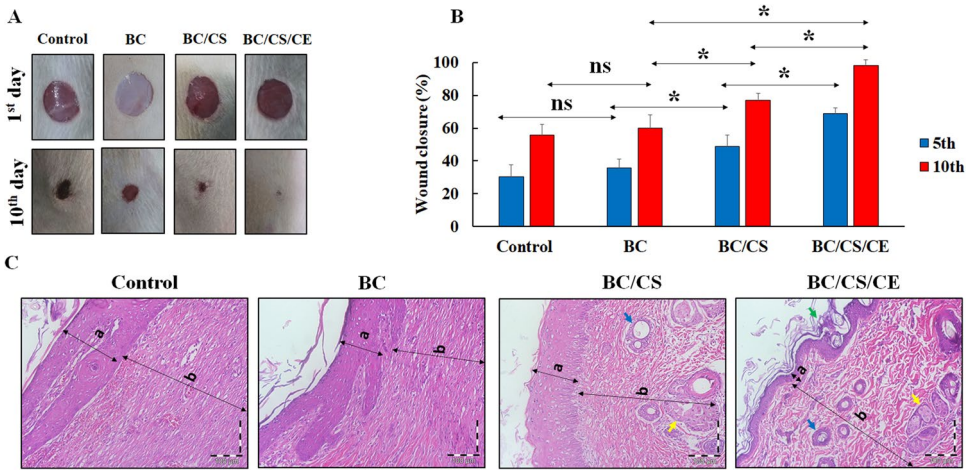

Fig. 6 (**A**) Macroscopic appearances of the wounds at the 1^{st} and 10^{th} day post-operation at control, BC, BC/CS, and BC/CS/CE groups. (**B**) Histograms of the wound closure percentages of the control, BC, BC/CS, and BC/CS/CE groups at the end of 5^{th} and 10^{th} day post-operation. The data are expressed as mean ± standard deviation (n = 8, *: $P < 0.05$, ns: not significant). (**C**) H&E stained sections of skin specimens from the wound site of the control, BC, BC/CS, and BC/CS/CE groups. Two-head arrows which are indicated by a and b letters exhibit epidermis and dermis layers, respectively. The green, blue, and yellow one-head arrows indicate the keratin layer, hair follicle, and sebaceous gland, respectively

by *Acetobacter xylinum,* and the wound dressing was fabricated by immersing the BC membranes in chitosan, followed by freeze-drying. They observed about 85% wound closure after 8 days, and the wounds were almost healed at 13th day after operation. It is apparent that our fabricated BC/CS/CE wound dressing exhibited more efficacy than the bacterial cellulose/chitosan membranes fabricated by Lin et al. as the wounds were completely healed at 10th day after their creation. Zhang et al. [60] fabricated a chitosan-collagen sponge and assessed it in the full-thickness excisional wound healing model of *Sprague Dawley* rats. They reported considerable wound healing after 14 days post-operation which is about 4 days more than the time needed for BC/CS/CE-treated wound to completely heal.

Conclusions

CS and CE were incorporated into the bacterial cellulose-based membranes. The BC/CS/CE membrane had significant biocompatibility with murine skin fibroblasts, sustained CE release profile, and appropriate mechanical properties. Besides, this composite membrane exhibited significantly higher antibacterial activity against *S. aureus* and *E. coli* compared with the BC and BC/CS membranes. Although the BC/CS/CE membrane exhibited high antibacterial efficacy in vitro, not using infected wounds models to assess the in vivo antibacterial efficacy of wound dressing was a limitation of this study. Moreover, the BC/CS/CE could significantly promote the healing process at the Wistar rats' skin excisions healing. Therefore, CS and CE incorporated bacterial cellulose-based membrane has a high ability to be used as an ideal wound dressing with remarkable antibacterial and wound healing activities. Further assessments of the efficacy of this wound dressing in the skin wound models of other species (e.g. rabbits, pigs, etc.) are a prerequisite of entering clinical trials.

Acknowledgements This research was supported by AJA University of Medical Sciences (97000961). This project is the replacement of my Compulsory military service so I should thanks the Iran's National Elites Foundation for this project.

Authors contribution The study was designed *by* A.K, R.H.F, and M.R. In vitro and in vivo assessments were carried out by A. K, R.H.F, M.R, E.H, and N.H.Y. The manuscript writing and revisions were done by A. K, M.R, and R.H.F. All the authors read and approved the manuscript before submission.

Data availability All datasets are available upon reasonable request.

Declarations

Conflict of interest The authors declare that they have no conflict of interest.

References

1. X. Zhao, H. Wu, B. Guo, R. Dong, Y. Qiu, P.X. Ma, Antibacterial anti-oxidant electroactive injectable hydrogel as self-healing wound dressing with hemostasis and adhesiveness for cutaneous wound healing. Biomater. **122**(1), 34–47 (2017)
2. X. Yang, W. Liu, N. Li, M. Wang, B. Liang, I. Ullah, A.L. Neve, Y. Feng, H. Chen, C. Shi, Design and development of polysaccharide hemostatic materials and their hemostatic mechanism. Biomater. Sci. **5**(12), 2357–2368 (2017)
3. K. Vig, A. Chaudhari, S. Tripathi, S. Dixit, R. Sahu, S. Pillai, V.A. Dennis, S.R. Singh, Advances in skin regeneration using tissue engineering. Int. J. Mol. Sci. **18**(4), 789 (2017)
4. S. Marquez-Bravo, I. Doench, P. Molina, F.E. Bentley, A.K. Tamo, R. Passieux, F. Lossada, L. David, A. Osorio-Madrazo, Functional bionanocomposite fibers of chitosan filled with cellulose nanofibers obtained by gel spinning. Polymers **13**(10), 1563 (2021)
5. G.D. Mogoşanu, A.M. Grumezescu, Natural and synthetic polymers for wounds and burns dressing. Int. J. Pharm. **463**(2), 127–136 (2014)
6. I. Sulaeva, U. Henniges, T. Rosenau, A. Potthast, Bacterial cellulose as a material for wound treatment: Properties and modifications A review. Biotechnol. Adv. **33**(8), 1547–1571 (2015)
7. D. Archana, B.K. Singh, J. Dutta, P.K. Dutta, Chitosan-PVP-nano silver oxide wound dressing. Int. J. Biol. Macromol. **73**, 49–57 (2015)
8. A. Khalid, H. Ullah, M. Ul-Islam, R. Khan, S. Khan, F. Ahmad, T. Khan, F. Wahid, Bacterial cellulose–TiO 2 nanocomposites promote healing and tissue regeneration in burn mice model. RSC Adv. **7**(75), 47662–47668 (2017)
9. N. Cai, C. Li, C. Han, X. Luo, L. Shen, Y. Xue, F. Yu, Tailoring mechanical and antibacterial properties of chitosan/gelatin nanofiber membranes with Fe3O4 nanoparticles for potential wound dressing application. Appl. Surf. Sci. **369**(30), 492–500 (2016)
10. M. Pang, Y. Huang, F. Meng, Y. Zhuang, H. Liu, M. Du, Q. Ma, Q. Wang, Z. Chen, L. Chen, Application of bacterial cellulose in skin and bone tissue engineering. Eur. Polym. J. **122**, 109365 (2020)
11. A.N. Frone, D.M. Panaitescu, C.A. Nicolae, A.R. Gabor, R. Trusca, A. Casarica, P.O. Stanescu, D.D. Baciu, A. Salageanu, Bacterial cellulose sponges obtained with green cross-linkers for tissue engineering. Mater. Sci. Eng. C **110**(1), 110740 (2020)
12. B. Wei, G. Yang, F. Hong, Preparation and evaluation of a kind of bacterial cellulose dry films with antibacterial properties. Carbohydr. Polym. **84**(1), 533–538 (2011)
13. S. Kumar, F. Ye, S. Dobretsov, J. Dutta, Chitosan nanocomposite coatings for food, paints, and water treatment applications. Appl. Sci. **9**(12), 2409 (2019)
14. K. Kalantari, A.M. Afifi, H. Jahangirian, T.J. Webster, Biomedical applications of chitosan electrospun nanofibers as a green polymer–Review. Carbohydr. Polym. **207**, 588–600 (2019)
15. M. Sadri, S. Arab-Sorkhi, H. Vatani, A. Bagheri-Pebdeni, New wound dressing polymeric nanofiber containing green tea extract prepared by electrospinning method. Fibers Polym. **16**(8), 1742–1750 (2015)
16. I. Bano, M. Arshad, T. Yasin, M.A. Ghauri, M. Younus, Chitosan: A potential biopolymer for wound management. Int. J. Biol. Macromol. **102**, 380–383 (2017)
17. S. Ahmed, S. Ikram, Chitosan & its derivatives: a review in recent innovations. Int. J. Pharm. Sci. Res. **6**(1), 14–30 (2015)
18. E.I. Rabea, M.E.-T. Badawy, C.V. Stevens, G. Smagghe, W. Steurbaut, Chitosan as antimicrobial agent: applications and mode of action. Biomacromol. **4**(6), 1457–1465 (2003)

19. T. Dai. M. Tanaka. Y. Y. Huang, M. R. Hamblin. Chitosan preparations for wounds and burns: antimicrobial and wound-healing effects. Expert Rev Anti Infect Ther. **9**(7), 857–879 (2011).
20. S. Aoyagi, H. Onishi, Y. Machida, Novel chitosan wound dressing loaded with minocycline for the treatment of severe burn wounds. Int J Pharm. **330**(1–2), 138–145 (2007)
21. R. Thakur, N. Jain, R. Pathak, S.S. Sandhu, Practices in wound healing studies of plants. Evid. Based Complement Alternat. Med. **20**(11), 438056 (2011)
22. K.I. Matshetshe, S. Parani, S.M. Manki, O.S. Oluwafemi, Preparation, characterization and in vitro release study of beta-cyclodextrin/chitosan nanoparticles loaded Cinnamomum zeylanicum essential oil. Int J Biol Macromol. **118**, 676–682 (2018)
23. Y. Zhang, X. Liu, Y. Wang, P. Jiang, S. Quek, Antibacterial activity and mechanism of cinnamon essential oil against Escherichia coli and Staphylococcus aureus. Health Scope **4**(4), 282–289 (2016)
24. O. Senhaji, M. Faid, M. Elyachioui, M. Dehhaoui, Antifungal activity of different cinnamon extracts. J. de Mycologie Medicale **15**(4), 220–229 (2005)
25. M. Raeisi, H. Tajik, A. Yarahmadi, S. Sanginabadi, Antimicrobial effect of cinnamon essential oil against Escherichia coli and Staphylococcus aureus. Health Scope (2015). https://doi.org/10.17795/jhealthscope-21808
26. I.S. Rana, A. Singh, R. Gwal, In vitro study of antibacterial activity of aromatic and medicinal plants essential oils with special reference to cinnamon oil. Int. J. Pharm. Pharm. Sci. **3**(4), 376–380 (2011)
27. G. Meades Jr., R.L. Henken, Constituents of cinnamon inhibit bacterial acetyl CoA carboxylase. Planta Med. **76**(14), 1570–1575 (2010)
28. M. Farahpour, M. Habibi, Evaluation of the wound healing activity of an ethanolic extract of Ceylon cinnamon in mice. Vet. Med. **57**(1), 53–57 (2012)
29. J.V. Kamath, A.C. Rana, A.R. Chowdhury, Pro-healing effect of Cinnamomum zeylanicum bark. Phytother. Res. **17**(8), 970–972 (2003)
30. A. Daemi, M. Lotfi, M.R. Farahpour, A. Oryan, S.J. Ghayour, A. Sonboli, Topical application of Cinnamomum hydroethanolic extract improves wound healing by enhancing re-epithelialization and keratin biosynthesis in streptozotocin-induced diabetic mice. Pharm. Biol. **57**(1), 799–806 (2019)
31. S. Ahmadi, A. Hivechi, S.H. Bahrami, P.B. Milan, S.S. Ashraf, Cinnamon extract loaded electrospun chitosan/gelatin membrane with antibacterial activity. Int. J. Biol. Macromol. **173**(15), 580–590 (2021)
32. J. Ahmed, E. Altun, M.O. Aydogdu, O. Gunduz, L. Kerai, G. Ren, M. Edirisinghe, Anti-fungal bandages containing cinnamon extract. Int. Wound J. **16**(3), 730–736 (2019)
33. A. Eskandarinia, A. Kefayat, M. Gharakhloo, M. Agheb, D. Khodabakhshi, M. Khorshidi, V. Sheikhmoradi, M. Rafienia, H. Salehi, A propolis enriched polyurethane-hyaluronic acid nanofibrous wound dressing with remarkable antibacterial and wound healing activities. Int. J. Biol. Macromol. **149**(15), 467–476 (2020)
34. W.-C. Lin, C.-C. Lien, H.-J. Yeh, C.-M. Yu, S.-h Hsu, Bacterial cellulose and bacterial cellulose–chitosan membranes for wound dressing applications. Carbohydr Polym. **94**(1), 603–611 (2013)
35. J.H. Ha, O. Shehzad, S. Khan, S.Y. Lee, J.W. Park, T. Khan, J.K. Park, Production of bacterial cellulose by a static cultivation using the waste from beer culture broth. Korean J. Chem. Eng. **25**(4), 812–815 (2008)
36. O. O. A., Use. Guidelines for Endpoints in Animal Study Proposals. (2011).
37. A. Eskandarinia, A. Kefayat, M. Agheb, M. Rafienia, M. Amini Baghbadorani, S. Navid, K. Ebrahimpour, D. Khodabakhshi, F. Ghahremani, A novel bilayer wound dressing composed of a dense polyurethane/propolis membrane and a biodegradable polycaprolactone/gelatin nanofibrous scaffold. Sci. Rep. **10**(1), 3063 (2020)
38. L.J. Bessa, P. Fazii, M. Di Giulio, L. Cellini, Bacterial isolates from infected wounds and their antibiotic susceptibility pattern: some remarks about wound infection. Int. Wound J. **12**(1), 47–52 (2015)
39. C. Kalirajan, P. Hameed, N. Subbiah, T. Palanisamy, A facile approach to fabricate dual purpose hybrid materials for tissue engineering and water remediation. Sci Rep. **9**(1), 1040 (2019)
40. P. Workman, E. Aboagye, F. Balkwill, A. Balmain, G. Bruder, D. Chaplin, J. Double, J. Everitt, D. Farningham, M. Glennie, Guidelines for the welfare and use of animals in cancer research. Br. J. Cancer **102**(11), 1555–1577 (2010)
41. J. Wallace, Humane endpoints and cancer research. ILAR J. **41**(2), 87–93 (2000)
42. K.E. Ibrahim, M.G. Al-Mutary, A.O. Bakhiet, H.A. Khan, Histopathology of the liver, kidney, and spleen of mice exposed to gold nanoparticles. Mol. **23**(8), 1848 (2018)
43. S. Yano, H. Maeda, M. Nakajima, T. Hagiwara, T. Sawaguchi, Preparation and mechanical properties of bacterial cellulose nanocomposites loaded with silica nanoparticles. Cellul **15**(1), 111–120 (2008)
44. M. Ul-Islam, N. Shah, J.H. Ha, J.K. Park, Effect of chitosan penetration on physico-chemical and mechanical properties of bacterial cellulose. Korean J. Chem. Eng. **28**(8), 1736–1743 (2011)
45. B. Soni, B. Hassan el, B. Mahmoud, Chemical isolation and characterization of different cellulose nanofibers from cotton stalks. Carbohydr. Polym. **134**, 581–589 (2015)
46. M. Fernandes Queiroz, K.R.T. Melo, D.A. Sabry, G.L. Sassaki, H.A.O. Rocha, Does the use of chitosan contribute to oxalate kidney stone formation? Mar. Drugs **13**(1), 141–158 (2015)
47. L.B. Gende, I. Floris, R. Fritz, MJ, Antimicrobial activity of cinnamon (Cinnamomum zeylanicum) essential oil and its main components against Paenibacillus larvae from Argentine. Bulletin of insectol. **61**(1), 1 (2008)
48. O. Shezad, S. Khan, T. Khan, J.K. Park, Physicochemical and mechanical characterization of bacterial cellulose produced with an excellent productivity in static conditions using a simple fed-batch cultivation strategy. Carbohydr. Polym. **82**(1), 173–180 (2010)
49. M. Litwiniuk, A. Krejner, M.S. Speyrer, A.R. Gauto, T. Grzela, Hyaluronic acid in inflammation and tissue regeneration. Wounds **28**(3), 78–88 (2016)
50. A. Eskandarinia, A. Kefayat, M. Rafienia, M. Agheb, S. Navid, K. Ebrahimpour, Cornstarch-based wound dressing incorporated with hyaluronic acid and propolis: In vitro and in vivo studies. Carbohydr. Polym. **216**(15), 25–35 (2019)
51. M.C. Robson, Wound infection. A failure of wound healing caused by an imbalance of bacteria. Surg. Clin. North Am. **77**(3), 637–650 (1997)
52. R.C. Goy, Dd. Britto, O.B. Assis, A review of the antimicrobial activity of chitosan. Polímeros. **19**, 241–247 (2009)
53. I.H. Hameed, H.J. Altameme, C. Mohammed, Evaluation of antifungal and antibacterial activity and analysis of bioactive phytochemical compounds of Cinnamomum zeylanicum (Cinnamon bark) using gas chromatography-mass spectrometry. Orient. J. Chem. **32**(4), 1769–1788 (2016)
54. S. Prabuseenivasan, M. Jayakumar, S. Ignacimuthu, In vitro antibacterial activity of some plant essential oils. BMC Compl. Alternat. Med. **6**(1), 1–8 (2006)
55. A.B. Hsouna, M. Trigui, R.B. Mansour, R.M. Jarraya, M. Damak, S. Jaoua, Chemical composition, cytotoxicity effect and antimicrobial activity of Ceratonia siliqua essential oil with preservative effects against Listeria inoculated in minced beef meat. Int. J. Food Microbiol. **148**(1), 66–72 (2011)

56. J. Sikkema, J.A. de Bont, B. Poolman, Mechanisms of membrane toxicity of hydrocarbons. Microbiol. Rev. **59**(2), 201–222 (1995)
57. G.I. Howling, P.W. Dettmar, P.A. Goddard, F.C. Hampson, M. Dornish, E.J. Wood, The effect of chitin and chitosan on the proliferation of human skin fibroblasts and keratinocytes in vitro. Biomater. **22**(22), 2959–2966 (2001)
58. I. Liakos, L. Rizzello, H. Hajiali, V. Brunetti, R. Carzino, P. Pompa, A. Athanassiou, E. Mele, J. Mater. Chem. B **3**(8), 1583–1589 (2015)
59. W.C. Lin, C.-C. Lien, H.-J. Yeh, C.-M. Yu, S.-h Hsu, Bacterial cellulose and bacterial cellulose–chitosan membranes for wound dressing applications. Carbohydr. Polym. **94**(1), 633–611 (2013)
60. M.X. Zhang, W.-Y. Zhao, Q.-Q. Fang, X.-F. Wang, C.-Y. Chen, B.-H. Shi, B. Zheng, S.-J. Wang, W.Q. Tan, L. Wu, Effects of chitosan-collagen dressing on wound healing in vitro and in vivo assays. J. Appl. Biomater. Funct. Mater. **19**, 1–10 (2021)